Design of a Calorimetric Facility to Asses Volumetric Receivers Employing a 42 kW High Flux Solar Simulator

Salvador Luque, José González-Aguilar and Manuel Romero

IMDEA Energy Institute, Avda. Ramón de la Sagra 3, 28935 Móstoles, Spain

Abstract

This paper presents the design of a new calorimetric facility for the experimental aerothermal assessment of volumetric receivers. The facility employs a 42 kW_e high flux solar simulator composed of 7 Xenon-arc lamps associated to as many ellipsoidal reflectors. An incident concentrated radiative power in excess of 14 kW_{th} is achieved at its focal point, with peak fluxes in excess of 3600 suns. A radiation homogenizer of square cross section is utilized upstream of the working section to uniformly heat the receiver aperture. Measured irradiance levels are discussed, and it is shown that the flow field non-dimensional governing parameters are highly representative of on-sun experiments at larger scales. The facility allows for the acquisition of comprehensive measurements to validate the design point operation of volumetric solar receivers, including absorber wall temperatures, air inlet and outlet temperatures, pressure drop, incident heat flux and thermal efficiency.

Keywords: Experimental Techniques, Performance Testing, Forced Convection, Thermal Radiation, Central Receiver Systems, Concentrating Solar Energy

1. Introduction

Solar receivers absorb incident concentrated sunlight and convert it to thermal energy at the temperature required by the downstream conversion process: mechanical, thermal, or chemical (Becker and Vant-Hull, 1991). To make them feasible for large-scale industrial deployment, it is expected that working fluid temperatures at receiver exit in excess of 720 ºC, thermal conversion efficiencies over 90%, minimum service life of 10,000 cycles, and overall costs below 150 USD per kilowatt of thermal power delivered ought to be achieved (Mehos et al, 2016). Operating temperatures play a conflicting role because receiver thermal losses typically become significant at the very high levels that are required for efficient downstream conversion processes.

Four heat transfer fluids have been researched in the development of solar power plants with central receiver systems: water (or steam, either saturated or subcritical), molten salts, sodium and air (Romero et al., 2002). The use of air has advantages in terms of abundance, availability, low environmental impact, and the ability to achieve very high temperatures without thermal degradation. In this context, volumetric receivers constitute a good alternative due to their functionality and geometric configuration. They operate as radiative-convective heat exchangers, generally at irradiance levels which can be approximately five times higher than those of tubular receivers (Romero et al., 2016). The goal is to achieve the so-called volumetric effect: a situation where the hottest part of the receiver is located deep inside its structure so that thermal emission losses from its outer surfaces (particularly the front face) are minimized (Boehmer et al., 1991).

Volumetric receivers are made of generally porous structures that enable concentrated sunlight to be absorbed and conducted within their solid volume, from where it is gradually transferred by forced convection to a heat transfer fluid that flows within (Ávila-Marín, 2011; Ho, 2017). Current design trends towards higher thermal efficiencies have led to the use of complex intricate geometries to maximize temperatures deep inside the structure and thus minimize frontal thermal emissions (Gómez-García et al., 2016). High (or selective) solar absorptance, high internal convective heat transfer, high (or directional) thermal conductivity, low radiative and convective thermal losses, mechanical durability at severe operating conditions, and, where possible,

Selection and/or peer review under responsibility of Scientific Committee
doi:10.18086/swc.2017.04.10 Available at http://proceedings.ises.org

inexpensiveness of manufacturing, operation and maintenance are all desired features for volumetric receivers.

There exists, to the authors' knowledge, scarce experimental evidence of solar receivers achieving a significant volumetric effect, the exception being a double-layer selective receiver composed of an external silica square-channel monolithic honeycomb (transparent in the solar spectrum and absorbent in the infrared band) and an internal layer of solar absorbent silicon carbide particles (Menigault et al., 1991). It is thus possible that selective reflectance and absorptance technologies (Kribus et al., 2014) or pressurized systems (Pozivil et al., 2015) are thus required.

This paper describes the design of a new calorimetric facility for the measurement of steady-state thermal conversion efficiency in volumetric receivers. The facility and its associated techniques are expected to serve as an experimental platform for the evaluation and validation of such radiative-convective heat exchangers in highly operation-representative conditions. Absorber samples up to a maximum aperture area of 300 cm^2 can be tested in it, at an incident power of 14 kW_{th}, typical air mass flow rates of 10 g/s, and maximum air outlet temperatures of approximately 1200 ºC. The facility allows for fully-integrated evaluations of performance and thermal conversion efficiency in solar receivers. Measurements acquired in it can thus be placed at technology readiness levels of 5 to 6 (technology validated and demonstrated in relevant environment).

2. The 42 kW High Flux Solar Simulator

High-flux solar simulators allow for the possibility of conducting high temperature solar thermal and thermochemical research under controlled, stable and adjustable laboratory conditions. The solar simulator employed in this study consists of 7 Xenon arc lamps, arranged in a compact hexagonal layout (Li et al., 2014). Cathodes and anodes are mounted on electrode rods, and contained within quartz glass bulbs. Each lamp is connected to a 6 kW electrical power supply and associated to an ellipsoidal reflector that also acts as a radiation concentrator. Reflectors are made from polished aluminum in order to have a very high reflectivity surface, in turn protected by a transparent polymeric coating. The ellipsoids have semi-major and semi-minor axes of 1374 mm and 569 mm, respectively, and their truncation diameter is 750 mm. The working section aperture plane is situated at a distance of 2314 mm from the reflector. The focal length is 2500 mm. The solar simulator has been illustrated in Fig. 1. Axisymmetric radiation flux profiles are achieved with this configuration, with peak flux in excess of 3600 kW/m^2 and a total incident power of approximately 14 kW_{th} at the working section aperture.

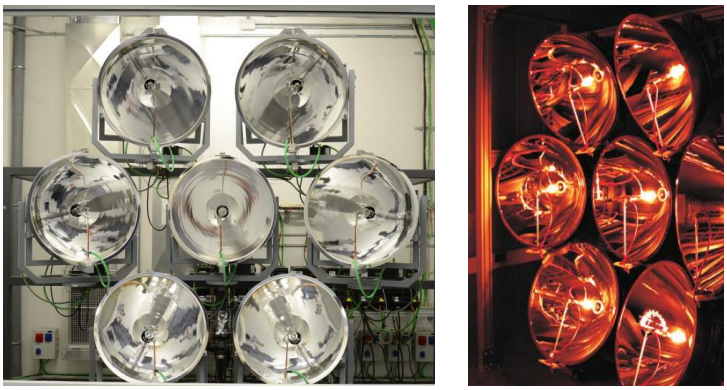

Fig. 1: Left, frontal photograph of the high flux solar simulator. Right, attenuated photograph of the Xenon lamps in operation

High flux solar simulators have the advantages of stable and adjustable radiation intensity and heat flux. They have been employed in research on high-temperature solar thermal applications, including solar thermo-chemistry, in the temperature range between 250 and 2250 ºC. Artificial radiation sources with spectral distributions that are close to that of actual sunlight are typically employed, such as metal halide lamps (Codd et al., 2010) and Xenon arc lamps (Petrasch et al., 2007; Krueger et al., 2011; Li et al., 2015). They are commonly employed in conjunction with ellipsoidal reflectors that concentrate radiation onto their secondary focal plane. Light sources and reflector surfaces are the main factors affecting the optical performance of high-flux solar simulators. The electric arc size has a notable influence on the optical performance of solar simulators. Smaller arcs allow for reflectors that are more effective at redirecting radiation toward the target focus. For this reason, Xenon arc lamps are typically preferred in the design and development of high-flux solar simulators.

3. Experimental Facility

A schematic diagram of experimental facility is given in Fig. 2. The facility is composed of the following elements: a fluid inlet module which also acts as a radiation homogenizer, a working section which houses the heavily thermally insulated receiver, an air-water heat exchanger to lower the air temperature to 50 °C, a thermal mass flow meter, a secondary air inlet for volumetric flow control, an air filter, and a high mass flow rate high pressure blower (operated by means of a frequency converter) that supplies the necessary pressure difference to circulate air through the system. Orifice plates of various sizes are employed to adjust the volumetric flow rate through the absorber between 5 and 20 g/s. They are installed in both primary and secondary air flow inlets in order to allow for adjustable pressure drops in both channels, which operate hydrodynamically in parallel. The facility is modular in design to allow for a rapid interchangeability of the test components, instrumentation, and experimental configurations.

The nominal operating mass flow rate through the absorber is 10 g/s, which leads to an average flow velocity in its flow channels of 2.8 m/s. The resultant Reynolds number is approximately 80, well inside de laminar flow regime. The pressure loss is thus, to first order, directly proportional to the mean flow velocity (and thus mass flow rates) in each flow channel. As non-uniform heating of volumetric absorbers can cause a reduction in their thermal conversion efficiency due to the dependence of air properties on temperature (which causes the air stream to flow preferentially through colder channels, where viscosity is lower), a radiation homogenizer is used to generate a uniform incident radiative heat flux on the absorber aperture. A 10 kW nominal shell-and-tube heat exchanger, operating in a counter-flow configuration, is utilized to lower the air temperatures from 1227 °C (achieved at the receiver outlet) to and 50 °C (suitable for operation of the downstream blower).

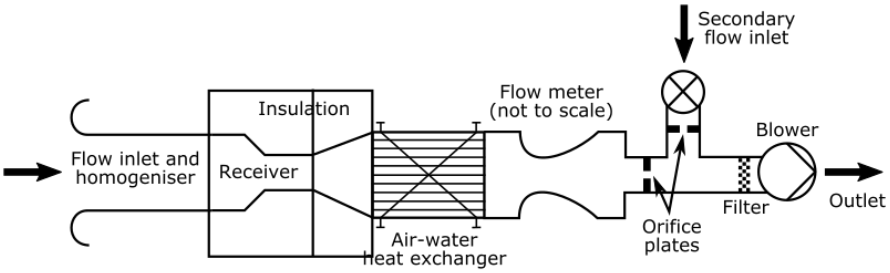

Fig. 2: Schematic diagram of the calorimetric experimental facility, with its main constitutive blocks labelled

Fig. 3: Left, frontal photograph of the absorber aperture plane (square lateral size is 125 mm). Right, three-dimensional view of the complete receiver, composed of the absorber plus a cup-shaped air collecting manifold

Two photographs of the baseline volumetric absorber experimentally characterized in this work are given in Fig. 3. It consists of a square-cell monolithic honeycomb module, manufactured from siliconized silicon carbide by Saint-Gobain High Performance Refractories[1], coupled to a cup that ducts the heated air towards the back of the facility. There are various experimental and numerical studies already conducted on this absorber (Téllez, 2003; Palero et al., 2008; Fend et al., 2013; Cagnoli et al., 2017), which therefore constitutes an adequate platform for the operational validation of new experimental facilities. The absorber has a 125 mm × 125 mm aperture and a

[1] Saint-Gobain IndustrieKeramik Rodental GmbH, Postfach 1144 D-96466 Rodental, Germany.

62.5 mm length. Absorber walls are 0.8 mm thick (nominal) and each flow channel is approximately 1.84 mm × 1.84 mm wide. The cross-sectional porosity of the absorber is thus 48.6%. Figure 4 illustrates the absorber assembly within the working section of the calorimetric facility. Sealing O-rings are distributed throughout the facility to prevent air leaks between the absorber aperture plane and the mass flow meter (such leaks would introduce unacceptably high uncertainties in the calculation of the absorber thermal conversion efficiency). During installation, the working section is placed on a highly accurate computer-controlled positioning table that moves along three axes. Careful alignment of the absorber aperture with the optical axis of the high flux solar simulator is achieved by employing a high precision cross level laser pointer. The inlet of the radiation homogenizer is situated exactly at focal point of the high flux solar simulator.

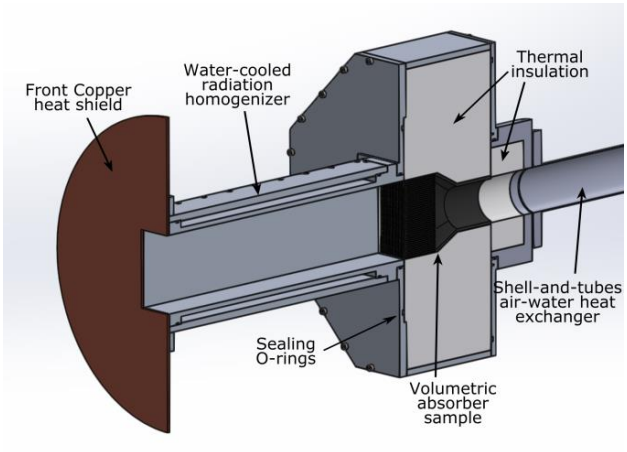

Fig. 4: CAD schematic diagram of the working section of the new experimental facility, with its main constitutive blocks labelled

4. Operating Conditions

A list of the operating conditions that can be achieved in the experimental facility is presented in Tab. 1, where comparisons to other experimental datasets at both smaller and larger scales are also given. Reynolds numbers have been calculated at the absorber aperture plane. Nusselt numbers and convective heat transfer coefficients have been obtained from correlations for thermal entry length solutions of the energy equation for internal laminar flows in square channels (Kays and Crawford, 2004). Averages have been taken along channel lengths.

Tab. 1: Typical operating conditions in the new experimental facility (at a scale of 42 kW_e) and comparison to values in the SolAir 200 on-sun experiments, from Téllez (2003), and to values achieved at a scale of 7 kW_e in a smaller solar simulator also at the Institute IMDEA Energy, reproduced from Luque et al. (2017)

Variable, units	7 kW_e scale	42 kW_e scale	SolAir 200
Absorber aperture, cm^2	4.5 – 9	156.3	2579
Total incident radiative power, kW	0.4 – 0.8	6.72	389
Maximum average radiation flux density, kW/m^2	1016	397.9	640
Mass flow rate, g/s	0.5 – 5	5 – 20	345
Mass flow rate per unit aperture area, $kg/(s\ m^2)$	1.3 – 2.1	0.7 – 2.6	~1.3
Maximum radiation per unit mass flow rate, kJ/kg	2500	1344	1128
Reynolds number (at inlet conditions)	50 – 250	62 – 248	~124
Average Nusselt number	3.0 – 3.24	3.02 – 3.15	~3.1
Average Biot number	0.52 – 2.92	0.57 – 2.27	~2.3
Technology readiness level (EU definition)	3 – 4	5 – 6	7 – 8

As shown in Tab. 1, the facility has been designed such that on-sun representative values of incident power per unit mass flow rate, Reynolds, Nusselt and Biot numbers can be achieved. Operating conditions that are highly representative of central receiver systems in actual solar towers are thus reproduced, whilst maintaining the advantages of operational flexibility and inexpensiveness of maintenance. The last row on the table shows technology readiness levels for the three experimental scales, based on the scale defined by the European Commission. The new experimental facility places itself between a smaller scale test bed for the aerothermal assessment of volumetric receivers already developed at the Institute IMDEA Energy (Luque et al., 2017), and actual on-sun central receiver experiments. It is thus expected that the flexibility and cost-effectiveness of the technique will allow for the validation of novel solar absorbers that show promise at the smaller scale, and prior to conducting on-sun tests, in order to de-risk the latter, typically resource-intensive, experimental campaign.

5. Instrumentation and Data Acquisition

The facility employs a dedicated instrumentation system based on an 8-slot National Instruments[1] CompactRIO platform. A total of 32 K-type thermocouples with 1 mm diameter Inconel sheaths have been placed throughout the facility, including measurement points on the radiation homogenizer walls and cooling water channels, on the intake module, on the absorber walls inner and outer walls, and in the exhaust module. Arrays of thermocouples were also placed at various position on the thermal insulating material in order to aid the calculation of heat conduction losses in it. The pressure drop across the absorber channels is measured by calibrated differential pressure transducers, and a thermal mass flow meter provides reliable mass measurement for the air flow.

Two radiation-shielded suction pyrometers are employed to accurately measure air inlet and outlet temperatures, immediately upstream and downstream of the absorber aperture and outlet planes, respectively. Their use is justified by the environment in which they operate and the fact that these measurements are key to the calculation of absorber thermal efficiency. Large amounts of radiation could affect unshielded thermocouples at those measurement planes: the radiation homogenizer outlet plane, where radiation from the high flux solar simulator is redirected and collimated, and the absorber exit plane, which is affected by intense thermal emissions from the hot inner walls of the facility.

A supervisory control and data acquisition system has been developed in National Instruments' LabVIEW for operation, hardware monitoring and data-logging in the experimental facility. Its main control window is shown in Fig. 5. It is divided in three main parts: on the left hand side, the user is presented with all control, monitoring and adjustment options for the 7 lamps of the high flux solar simulator. All information related to the facility instrumentation is displayed on the top right of the screen. Finally, the right lower part contains all options for the control and automated motion of the high precision three-axis positioning table. Safety operation interlocks have been included in the program to prevent hardware damage through user error.

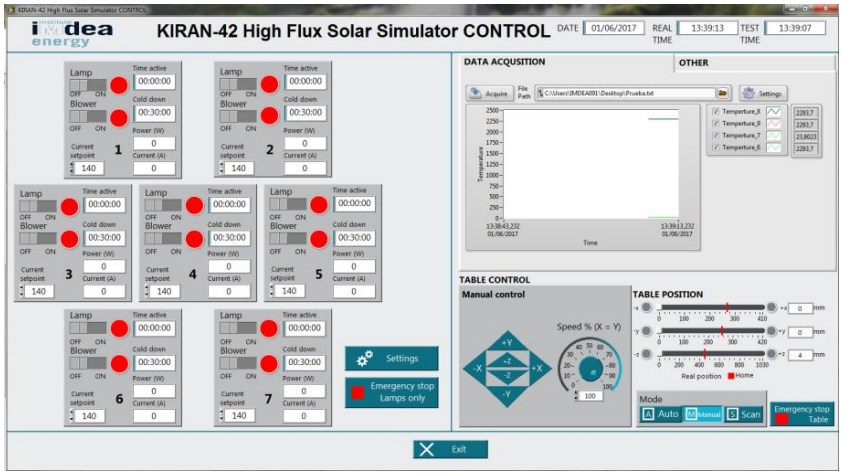

Fig. 5: Captured screen of the supervisory control and data acquisition (SCADA) software

[1] National Instruments Corporation, 11500 N Mopac Expy, Austin, Texas 78759, USA.

6. Radiation Conditioning on Absorber Aperture

Non-uniform heating of volumetric absorbers can cause a reduction in their thermal conversion efficiency (Pitz-Paal et al. 1997). The dependence of air properties on temperature causes the air stream to flow preferentially through colder channels, where viscosity is lower. Hotter flow channels then remain relatively uncooled, and the temperature imbalance can lead to a runaway effect that originates flow instabilities and hot spots on the absorber aperture. Orifice plates can be used to balance the flow by creating additional pressure loss in colder flow channels. When designing an experimental facility, a well-conditioned set-up requires the use of radiation homogenizers to produce a uniform incident heat flux on the absorber aperture.

Numerical ray-tracing simulations were then conducted during the design of the radiation homogenizer with the objective of maximizing the uniformity of the radiation profile at its outlet plane. The 7-lamp high flux solar simulator and the homogenizer were modelled in Tracepro[1]. The homogenizer was assumed to be a square cross-sectioned tube with a length of 500 mm and height and width both equal to 125 mm in this analysis. The mirrors were defined as perfect reflectors as the main goal was to assess the uniformity of radiation profiles rather than obtain actual values. In the ray-tracing simulation 100,000 rays per lamp were calculated, assumed to be emitted by a surface source located at the first focal point of each ellipsoidal reflector. The homogenizer inlet plane is situated exactly at the second focal point of the ellipsoidal reflectors.

Figure 6 shows the irradiance distribution on the outlet plane of the homogenizer, normalized with respect to the peak flux. The graph on the left hand side have been smoothed and averaged in groups of 8×8 pixels. The graphs in the middle show normalized heat flux profiles in the horizontal and vertical directions. On the right hand side the simulated rays are displayed in the setup. The analysis was conducted for all seven lamps both individually and in conjunction, but only selected results are shown for brevity. The simulations showed that moving the homogenizer closer to the ellipsoidal reflectors (i.e., ahead of the solar simulator focal point) results in a slightly smoother profile in horizontal direction, but a lower radiation level in the vertical direction. Moving the homogenizer away from the reflectors leads to an inverse horizontal profile, i.e., one where regions of maximum heat flux are found near the corners rather than in the center.

Single lamp analyses showed small areas in the center of the homogenizer outlet plane where irradiance was relatively lower than in their surroundings. This can be explained by the existence of a hole in the center of each the ellipsoidal reflector through which the lamp bulb electrical connections pass through. Simulations showed that these troughs could be reduced by moving the homogenizer away from the solar simulator focal point, but this led, again, to inverse radiation profiles. On the basis of this study, the final decision was to operate the radiation homogenizer with its inlet plane located exactly on the solar simulator focal plane. Numerical results showed that this configuration provided the best balance between homogeneity of the heat flux profiles and overall incident power on the absorber aperture.

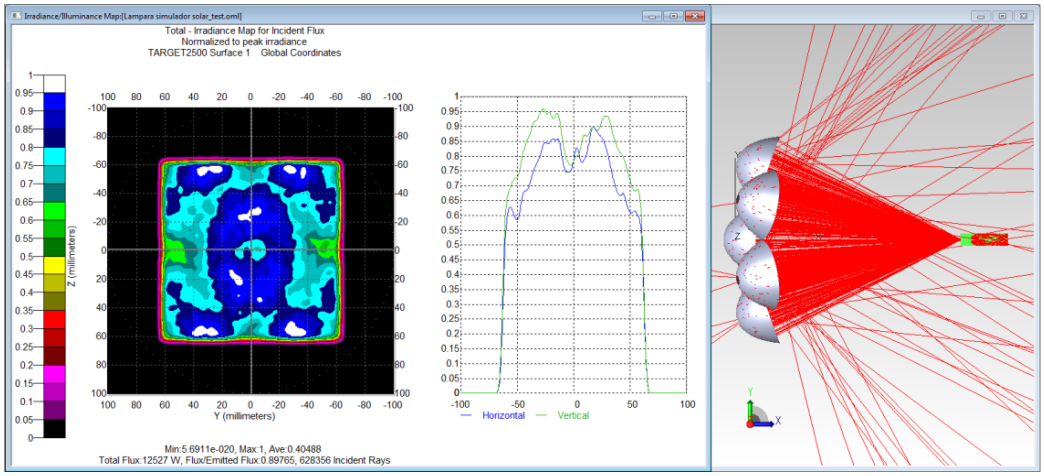

Fig. 6: Left, normalized heat flux map at the homogenizer outlet plane, for all seven lamps of the solar simulator. Center, normalized radiation profiles along the horizontal and vertical directions. Right, image of the simulated rays.

[1] Lambda Research Corporation, 25 Porter Road, Littleton, MA 01460, USA.

7. Incident Radiation Flux Distribution

The radiative flux density distribution at the outlet plane of the radiation homogenizer was acquired by direct measurements conducted with a Gardon radiometer (Gardon, 1953). The gauge traverses the measurement plane by means of an automated motion control mechanism that allows for high-spatial measurement resolution. At the homogenizer inlet plane, on the contrary, heat flux measurements were acquired by employing a water-cooled Lambertian target, in a procedure which was described in detail by Li et al. (2014). Radiation intensity on the Lambertian target was recorded by employing a high resolution CCD camera, which was calibrated against the Gardon radiometer.

Irradiance maps at the inlet and outlet of the radiation homogenizer are shown in Fig. 7. The white line in the right hand side figure indicates the actual size and relative location of the volumetric absorber aperture plane. It can be observed that the highly non-uniform and approximately Lorentzian radiation profile produced by the high-flux solar simulator is transformed to a square and relatively flat profile at the homogenizer outlet. The uniformity of the irradiance map at the homogenizer outlet was characterized by an average of 397.9 kW/m^2 and a standard deviation of 136.4 kW/m^2, both measured over a surface area of 125 mm × 125 mm (equal to the absorber aperture). The peak flux is 607.6 kW/m^2. Integration leads to an overall incident radiative power on the homogenizer outlet of 6.72 kW$_{th}$. This plane is approximately 2 mm upstream of the absorber aperture, so uniform heating of its front face is considered to be achieved.

There are, nonetheless, slight discrepancies with respect to results from the numerical ray-tracing simulations, especially noticeable in the region of high heat flux near the geometric center of the homogenizer outlet and the radiation trough that is found in the upper region of the channel (Fig. 7, right). This is attributed to two main effects: first, having a less reflective homogenizer than simulated, which leads to a lower level of homogenization of the outlet heat flux, and, second, to slight misalignments in the solar simulator with respect to the perfectly aligned numerically simulated configuration. Measurements showed that the points of maximum heat flux of all seven lamps where contained within a circular area of 18 mm diameter, whereas the simulation assumed perfect concentric alignment.

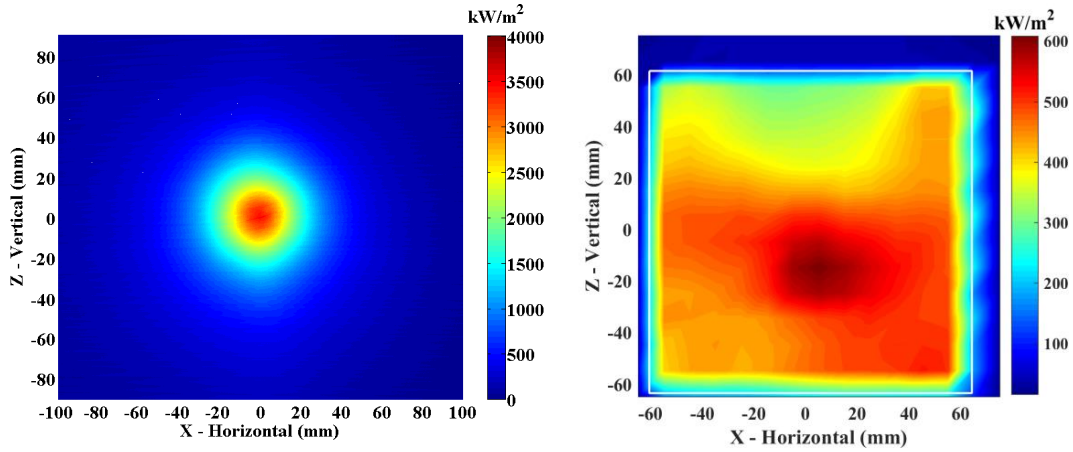

Fig. 7: Left, measurements of irradiance at the homogenizer inlet plane, reproduced from Li et al. (2014). Right, measurements of irradiance at the homogenizer outlet plane, conducted by traversing a Gardon radiometer

Laterally averaged irradiance distributions at the homogenizer inlet and outlet planes are shown in Fig. 8. Two curves are shown in the figure, one for Z-averaged data (in which averages have been taken along the vertical direction), and one for X-averaged data (in which averages have been taken along the horizontal direction). The edges of the absorber aperture are located at -62.5 mm and 62.5 mm. It can be observed that the X-averaged data shows the region of high heat flux that is close to the center of the absorber aperture, as well as the trough on the upper part. Z-averaged measurements presented in Fig. 8 also show a somewhat higher irradiance towards the right hand side of the absorber aperture.

In assessing whether or not the heat flux distribution on the absorber aperture can lead to the unstable operation of volumetric receivers, the receiver thermal conductivity was also shown to be an important factor to consider by Becker et al. (2006). In a theoretical and numerical study, it was demonstrated that sufficiently conductive

volumetric receivers could altogether avoid flow instabilities by allowing for an enhanced redistribution of heat within the absorber solid volume. As a result, the temperature difference between hot and cold flow channels is not sufficient for instabilities to occur. Considering that the volumetric absorber to be tested is made out of highly conductive siliconized silicon carbide, the heat flux profile at the homogenizer outlet was thus considered sufficient for the stable operation of the experimental facility in this initial aerothermal characterization test campaign.

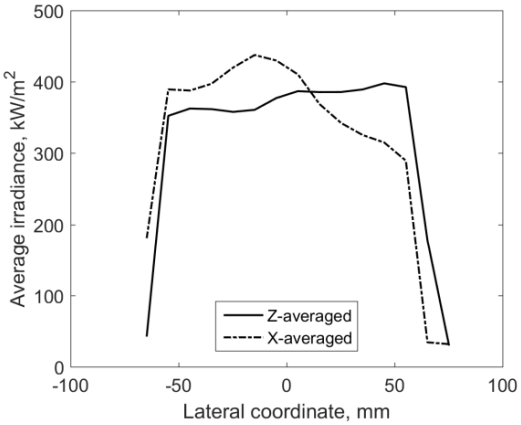

Fig. 8: Laterally averaged irradiance distributions at the radiation homogenizer outlet plane

8. Conclusions

A new calorimetric facility has been designed to investigate volumetric absorbers by employing a seven-lamp 42 kW high flux solar simulator, and is described in this paper. A modular design has been sought to allow for the quick interchangeability of components and experimental configurations. Incident radiation levels and internal flow field variables have been shown to be highly representative of central receiver systems in actual solar towers. Together with its associated techniques, the facility allows for fully integrated assessments of absorber radiative-to-convective heat conversion efficiencies, whilst maintaining the advantages of operational flexibility and inexpensiveness of maintenance.

It is envisaged that the facility will be used in investigations of novel volumetric absorbers that include gradual variations of convective heat transfer coefficients (implemented, for instance, by variable porosity configurations), gradual variations of thermal conductivity through the sample, or selective absorptance and reflectance profiles. Transient measurements are possible too. The technique is expected to allow for a more rapid experimental validation of such innovative concepts than has previously been possible. Experimental data will also be used for the validation of both high-fidelity numerical simulations and simplified analytical models of air solar receivers in high-irradiance high-temperature operation. Besides, the new facility can also serve as a platform for the validation of other type of central receiver systems for concentrated solar power applications, (for instance directly or indirectly heated tube and particle receivers) with minimal changes to the experimental apparatus.

9. Acknowledgements

Research leading to these results has received funding from the regional government of Comunidad de Madrid through project ALCCONES (S2013/MAE-2985), and from the European Union FP7 Programme through grant agreements 609837 and REA 291803 (Marie Curie Actions). Lena Bühre is thanked for substantial contributions relating to the radiation homogenizer numerical ray-tracing simulations. All are gratefully acknowledged.

10. References

Ávila-Marín, A.L., 2011. Volumetric receivers in solar thermal power plants with central receiver system technology: a review. Solar Energy 85(5), 891-910.

Becker, M., Vant-Hull, L., 1991. Thermal Receivers, in: Solar power plants. Berlin Heidelberg: Springer, pp. 163–198.

Becker, M., Fend, T., Hoffschmidt, B., Pitz-Paal, R., Reutter, O., Stamatov, V., Steven, M., Trimis, D., 2006. Theoretical and numerical investigation of flow stability in porous materials applied as volumetric solar receivers. Solar energy 80(10), 1241-1248.

Boehmer, M., Becker, M., and Sánchez, M., 1991. Development of volumetric air receivers, in: Proceedings of the Biennial Congress of ISES, Pergamon Press, Denver, Colorado, USA, pp. 2123-2128.

Cagnoli, M., Savoldi, L., Zanino, R., Zaversky, F., 2017. Coupled optical and CFD parametric analysis of an open volumetric air receiver of honeycomb type for central tower CSP plants. Solar Energy 155, 523-536.

Codd, D. S., Carlson, A., Rees, J., Slocum, A. H., 2010. A low cost high flux solar simulator. Solar Energy 84(12), 2202-2212.

Fend, T., Schwarzbözl, P., Smirnova, O., Schöllgen, D., Jakob, C., 2013. Numerical investigation of flow and heat transfer in a volumetric solar receiver. Renewable energy 60, 655-661.

Gardon R., 1953. An instrument for the direct measurement of intense thermal radiation. Rev. Sci. Instrum. 24(5), 366-370.

Gómez-García, F., González-Aguilar, J., Olalde, G., Romero, M., 2016. Thermal and hydrodynamic behavior of ceramic volumetric absorbers for central receiver solar power plants: A review. Renewable Sustainable Energy Rev. 57, 648-658.

Ho, C.K., 2017. Advances in central receivers for concentrating solar applications. Solar Energy 152, 38-56.

Kays W, Crawford M, Weigand B., 2004. Convective heat and mass transfer, fourth ed. McGraw-Hill Higher Education, New York, NY, USA.

Kribus, A., Gray, Y., Grijnevich, M., Mittelman, G., Mey-Cloutier, S., Caliot, C., 2014. The promise and challenge of solar volumetric absorbers. Solar Energy 110, 463-481.

Krueger, K. R., Davidson, J. H., Lipinski, W., 2011. Design of a new 45 kWe high-flux solar simulator for high-temperature solar thermal and thermochemical research. J. Solar Energy Eng. 133(1), 011013.

Li, J., González-Aguilar, J., Pérez-Rábago, C., Zeaiter, H., Romero, M., 2014. Optical analysis of a hexagonal 42 kW_e high-flux solar simulator. Energy Procedia 57, 590-596.

Li, J., González-Aguilar, J., Romero, M., 2015. Line-concentrating flux analysis of 42 kW_e high-flux solar simulator. Energy Procedia 69, 132-137.

Luque, S., Bai, F., González-Aguilar, J., Wang, Z., Romero, M., 2017. A parametric experimental study of aerothermal performance and efficiency in monolithic volumetric absorbers, in: AIP Conference Proceedings, 1850, 030034.

Luque. S., Santiago, S., Gómez-García, F., Romero, M., González-Aguilar, J., 2017. A new calorimetric facility to investigate radiative-convective heat exchangers for concentrated solar power applications. Int. J. Energy Res. X, 1-11.

Mehos, M., Turchi, C., Jorgenson, J., Denholm, P., Ho, C., Armijo, K., 2016. On the path to Sunshot: advancing concentrating solar power technology, performance, and dispatchability. Tech. Rep. NREL/TP-5500-65688, National Renewable Energy Laboratory, Golden, Colorado, USA.

Menigault, T., Flamant, G., Rivoire, B., 1991. Advanced high-temperature two-slab selective volumetric receiver. Solar energy materials 24(1-4), 192-203.

Palero, S., Romero, M., Castillo, J.L., 2008. Comparison of experimental and numerical air temperature distributions behind a cylindrical volumetric solar absorber module. J. Solar Energy Eng. 130(1), 011011.

Petrasch, J., Coray, P., Meier, A., Brack, M., Häberling, P., Wuillemin, D., Steinfeld, A., 2007. A novel 50 kW 11,000 suns high-flux solar simulator based on an array of Xenon arc lamps. J. Solar Energy Eng. 129(4) 405-411.

Pitz-Paal. R., Hoffschmidt, B., Boehmer, M., Becker, M., 1997. Experimental and numerical evaluation of the performance and flow stability of different types of open volumetric absorbers under non-homogeneous irradiation. Solar Energy 60, 135-150.

Pozivil, P., Ettlin, N., Stucker, F., Steinfeld, A., 2015. Modular design and experimental testing of a 50 kWth pressurized-air solar receiver for gas turbines. J. Solar Energy Eng. 137(3), 1-7.

Romero, M., Buck R., Pacheco, J.E., 2002. An update on solar central receiver systems, projects, and technologies. J. Solar Energy Eng. 124(2), 98-108.

Romero, M., González-Aguilar, J., Zarza, E., 2016. Concentrating solar thermal power, in: Goswami, D.Y., Kreith, F. (Eds.), Energy efficiency and renewable energy handbook, second ed. CRC Press, Boca Raton, Florida, USA, pp. 1237-1345.

Téllez, F.M., 2003. Thermal performance evaluation of the 200 kW_{th} "SolAir" volumetric solar receiver. Tech. Rep. 1024, CIEMAT (Centro de Investigaciones Energéticas, Medioambientales y Tecnológicas), Almería, Spain.